Enhanced Mediterranean water cycle explains increased humidity during MIS 3 in North Africa

Mike Rogerson[1]

Yuri Dublyansky[2]

Dirk L. Hoffmann[3]

Marc Luetscher[2,4]

Paul Töchterle[2]

Christoph Spötl[2]

1 School of Environmental Sciences, University of Hull, Cottingham Road, Hull, HU6 7RX, UK.

2 Institute of Geology, University of Innsbruck, Innrain 52, 6020 Innsbruck, Austria.

3 Department of Human Evolution, Max Planck Institute for Evolutionary Anthropology, Deutscher Platz 6, 04103, Leipzig, Germany

4 Swiss Institute for Speleology and Karst Studies (ISSKA), Serre 68, CH-2300 La Chaux-de-Fonds

Abstract

We report a new fluid inclusion dataset from Northeast Libyan speleothem SC-06-01, which is the largest speleothem fluid inclusion dataset for North Africa to date. The stalagmite was sampled in Susah cave, a low altitude coastal site, in Cyrenaica, on the northern slope of the Jebel Al-Akhdar. Speleothem fluid inclusions from latest Marine Isotope Stage (MIS) 4 and throughout MIS 3 (~67 to ~30 ka BP) confirm the hypothesis that past humid periods in this region reflect westerly rainfall advected through the Atlantic storm track. However, most of this moisture was sourced from the Western Mediterranean, with little direct admixture of water evaporated from the Atlantic. Moreover, we identify a second moisture source likely associated with enhanced convective rainfall within the Eastern Mediterranean. The relative importance of the western and eastern moisture sources seems to differ between the humid phases recorded in SC-06-01. During humid phases forced by precession, fluid inclusions record compositions consistent with both sources, but the 52.5 – 50.5 ka interval forced by obliquity reveals only a western source. This is a key result, showing that although the amount of atmospheric moisture advections changes, the structure of the atmospheric circulation over the Mediterranean does not fundamentally change during orbital cycles. Consequently, an arid belt must have been retained between the Intertropical Convergence Zone and the mid-latitude winter storm corridor during MIS 3 pluvials.

Introduction

Atmospheric latent heat is a major component of global and regional climate energy budgets and changes in its amount and distribution are key aspects of the climate system (Pascale et al., 2011). Equally, in mid- and low-latitude regions, changes in the water cycle have more impact on landscapes and ecosystems than changes in sensible heat (Black et al., 2010). Rainfall in semi-arid regions is thus one of the key climate parameters that understanding future impact on human societies depends upon (IPCC, 2014), making constraining of mid-latitude hydrology a globally significant research priority. These regions, however, have a particularly sparse record of palaeoclimate due to typically poor preservation of surface sedimentary archives (Swezey, 2001). North Africa is a region that fully

exhibits these limitations, and large areas present either no pre-Holocene record or else they present highly discontinuous deposits indicating major reorganisation of the hydroclimate, which are challenging to date (Armitage et al., 2007). North Africa also fully exhibits the progress palaeoclimatologists have made in understanding continental hydrological change from its impact on the marine system; our understanding of past North African hydroclimate is disproportionately drawn from records from the Mediterranean Sea (Rohling et al., 2015) and the eastern Central Atlantic (Goldsmith et al., 2017;deMenocal et al., 2000.;Adkins et al., 2006).

Past changes in North African hydroclimate

Marine-based evidence offers a coherent model in which changes in the spatial distribution of insolation alter atmospheric circulation on orbital timescales (10^4 to 10^5 years) and force major reorganisations of rainfall in semi-arid regions such as the Sahel and southern Saharan regions (Rohling et al., 2015;Goldsmith et al., 2017). This result is at least partially confirmed in climate modelling experiments (Bosmans et al., 2015;Tuenter et al., 2003) and provides a conceptual framework in which fragmentary evidence of hydrological change on the adjacent continent can be understood (Rowan et al., 2000). There is 1) strong geochemical evidence that runoff from the African margin initiated the well-known "sapropel" thermohaline crises of the eastern Mediterranean (Osborne et al., 2010;Osborne et al., 2008) and, 2) convincing evidence that the southern margin of the Mediterranean was more variable than the northern in terms of the relative magnitude of precipitation changes and the distribution of flora, fauna and hominid populations (Drake et al., 2011). However, we emphasise the fact that this understanding is largely drawn from evidence from outside continental North Africa, and that this limits our knowledge about the nature and impact of hydrological changes in this region.

There is strong evidence for a more humid climate throughout the Sahara and Sahel regions during the early Holocene (Gasse and Campo, 1994;Gasse, 2002;Fontes and Gasse, 1991;Prentice and Jolly, 2000;Jolly et al., 1998;Collins et al., 2017), and in older interglacial periods (Drake et al., 2008;Armitage et al., 2007;Vaks et al., 2013). This evidence has been interpreted to indicate that humid conditions extended from the modern Sahel (~15^{o}N) to the Mediterranean coast (30-35^{o}N).

However, this only partially agrees with model results, which do indicate orbitally forced migration of the monsoon belt but not across such a large spatial scale as suggested by the empirical data. Model experiments indicate that monsoonal rainfall occurring within the Intertropical Convergence Zone (ITCZ) likely extended no further north than ~23°N (Harrison et al., 2015). This well-recognised lack of agreement between rainfall fields in model experiments for the past and reconstructed hydrographies from the distribution of lakes and vegetation (via pollen) (Peyron et al., 2006) remains a major research problem. While some models also suggest that during times of high Northern Hemisphere insolation, enhanced westerlies advected Atlantic moisture into the basin (Brayshaw et al., 2009;Tuenter et al., 2003;Bosmans et al., 2015), high-resolution regional modelling indicates that this primarily affected the northern Mediterranean margin only (Brayshaw et al., 2009). This result is consistent with evidence of enhanced runoff at these times from the southern margin of Europe (Toucanne et al., 2015). On the African coast east of Algeria, the southern limit of enhanced precipitation arising from increased westerly activity within model experiments essentially lies at the coastline (~32°N), and does not appear to drive terrestrial hydrological changes. Overall, there is therefore a striking mismatch between the apparent humidity of Africa between 23 and 32°N in the empirical record (a zonally oriented belt ~1000 km in width) and the climate models. This region encompasses southern Tunisia, in which multiple lines of evidence for distinct and widespread periods of increased humidity provide a highly secure basis for enhanced rainfall during Northern Hemisphere insolation maxima (Ballais, 1991;PETIT-MAIRE et al., 1991), the Fezzan basin, in which compelling evidence for multiple lake highstands exists (Drake et al., 2011) and western Egypt, where large tufa deposits attest to higher past groundwater tables (Smith et al., 2004).

An emerging picture of MIS 3 as a humid period within the Mediterranean basin is developing (Langgut et al., 2018), and the current study focusses on this time period. However, MIS 3 is not well expressed in the Sahara region. The Libyan interior is considered arid or even hyperarid throughout the last glacial period (Cancellieri E. et al., 2016). Recent re-evaluation of palaeolake levels in southwest Egypt indicates a groundwater-fed system active around 41 ka (Nicoll, 2018), which is similar to dates for springline tufa systems at Kharga Oasis (Smith et al., 2007). We are not aware of

continental MIS 3 pollen records from the region, but marine pollen from Tunisia indicates more arid conditions through the last glacial than during the Holocene (Brun, 1991). There is a triple peak in runoff from the Nile recorded in the marine sediment record, with maxima at ~60, ~55 and ~35 ka, indicating higher rainfall within the upper Nile catchment (Revel et al., 2010).

It is unlikely that significant further progress will be made in understanding the palaeoclimate of North Africa without new empirical evidence of regional hydrological changes from which atmospheric dynamics can be delineated.

The central North African speleothem record

Speleothem palaeoclimatology has high potential for North Africa, but is only recently becoming established through key records developed for Morocco (Wassenburg et al., 2013;Ait Brahim et al., 2017;Wassenburg et al., 2016). Until recently, the only speleothem record published from central North Africa was a single continuous record from 20 to 6 ka BP from northern Tunisia (Grotte de la Mine). This record shows a large deglacial transition in both $\delta^{13}C$ and $\delta^{18}O$ (Genty et al., 2006), with oxygen isotopes indicating a 2-step change from a relatively isotopically heavy (-5‰) LGM (20-16 ka BP), through an intermediate (-6 to -7‰) deglacial period (16-11.5 ka BP) to a relatively isotopically light early Holocene. The $\delta^{13}C$ record indicates cool periods exhibiting higher carbon isotope values, more clearly delineating the Bølling-Allerød / Younger Dryas oscillation than $\delta^{18}O$. This is assumed to reflect higher soil respiration during warm periods (Genty et al., 2006). A major change in the carbon isotopic composition occurred across the transition from the relatively arid glacial to the more humid Early Holocene, and indicates a significant reorganisation of the regional hydroclimate. However, it is difficult to interpret these data in isolation. A recently reported speleothem record (SC-06-01) indicates that conditions in northern Libya during Marine Isotope Stage 3 (MIS 3) were more humid than today, and shows isotopic evidence of a teleconnection between temperature in Greenland and rainfall at the southern Mediterranean margin (Hoffmann et al., 2016). The oxygen isotope record indicates that the water dripping into the cave during MIS 3 was isotopically too heavy for the moisture to be sourced from within the monsoon system (Hoffmann et al., 2016). However, beyond ruling out a southern source $\delta^{18}O_{cc}$ values alone are not sufficient to determine the origin of

atmospheric vapour. Three distinct humid phases within MIS3 are reported from this speleothem: 65-61 ka, 52.5-50.5 ka and 37.5-33 ka. Phases I and III occur during times of low precession parameter, when summer insolation on the northern hemisphere is relatively increased. Phase II represents the first evidence for high obliquity being able to cause a pluvial period in the north African subtropics in the same manner as precession (Hoffmann et al., 2016). In SC06-01, all three growth phases are fractured into multiple short periods of growth, and show a marked temporal coherence with Greenland Dansgaard-Oeschger interstadials (Hoffmann et al., 2016). Here, we report fluid inclusion data from this speleothem and discuss how this helps resolve some of the issues discussed above.

Fluid Inclusions

Speleothem fluid inclusions are small volumes of water that were enclosed between or within calcite crystals as they grew, ranging in size from less than 1 μm to hundreds of μm (Schwarcz et al., 1976). This water represents quantities of ancient drip-water that can be interrogated directly to ascertain the isotopic properties of the oxygen ($\delta^{18}O_{fi}$) and hydrogen ($\delta^{2}H_{fi}$) it comprises. This powerful approach circumvents some of the uncertainty inherent in the interpretation of the stable isotopic values preserved in the calcite comprising the speleothem itself ($\delta^{18}O_{cc}$, $\delta^{13}C_{cc}$). Fluid inclusion isotopes have been used to demonstrate changes in air temperatures (Wainer et al., 2011;Meckler et al., 2015;Arienzo et al., 2015) and in the origin of the moisture from which precipitation was sourced (McGarry et al., 2004;Van Breukelen et al., 2008). Fluid inclusions from speleothems in Oman have also been used to identify monsoon-sourced precipitation during interglacial phases (Fleitmann et al., 2003), providing a rationale for similar investigation of fluid inclusion isotope behaviour in North Africa.

In the case of fluid inclusions from northeastern Libyan speleothems, the boundary conditions for atmospheric moisture supply are 1) the sea-surface temperature of the Atlantic and Mediterranean, 2) the surface water $\delta^{18}O_{sw}$ of the same ocean regions, 3) land surface temperature of Africa and to a lesser extent southern Europe, 4) insolation (especially with respect to ITCZ position) and 5) the zonal pressure gradient across northern Africa.

Modern rainfall system

Modern rainfall in central North Arica is dominated by relatively wet winters, and summers with little, if any, precipitation. Convective systems, cyclones, upper-level troughs and static instabilities can all drive rainfall patterns in the Mediterranean basin and these modes are reviewed in (Dayan et al., 2015). Convection essentially reflects the relatively high SST of the Mediterrnaean during the winter, but rising air masses generally also need significant advection of moisture to drive significant rainfall. Upper level troughs reflect large-scale circulation (e.g. Red Sea Trough) or reflect lee effects downstream of mountains in the western Mediterranean, and promote rainfall in their regions of formation. The dominant cyclogenic centre is in the Gulf of Genoa, and secondary centres are placed in south Italy, Crete and Cyprus. Cyclonic systems can also penetrate from the Atlantic, where the high SST of the winter Mediterranean tends to sustain and amplify them, in close analogy to convection forcing. The key static instability is the penetration of the tropical air mass into the subtropical Mediterranean, forming a 'Saharan Cloud Band' at middle and upper atmospheric levels. These originate from within the ITCZ. Libya is very sparsely instrumented, so we assume that synoptic processes are similar to the Levant region. Here, most rainfall falls under winter, low pressure conditions, and is convective (Peleg and Morin, 2012). The responsible low pressure systems can relate to transient, shallow lows north of the area in which rainfall is occurring, or less frequently more long-lasting Cyprus Lows or Red Sea Trough systems (Peleg and Morin, 2012).

Material and Methods

SC-06-01 is a 93-cm long stalagmite from Susah Cave (Fig. 1, 32°53.419' N, 21°52.485' E), which lies on a steep slope ~200 m above sea level in the Al Akhdar massif in Cyrenaica, Libya (Fig. 1). The region is semi-arid today, with mean annual temperature ~20°C and receiving less than 200 mm precipitation per year, mostly in the winter (October to April). The Al Akhdar massif has thin soil cover and a Mediterranean "maquis" vegetation. Susah Cave is hydrologically inactive today, and all formations are covered with dust. The chronology of the speleothem and the general features of its growth and $\delta^{18}O_{cc}$ record are published elsewhere (Hoffmann et al., 2016), and this study focuses on

fluid inclusion isotopes, their impact on the interpretation of $\delta^{18}O_{cc}$ and to a lesser extent on $\delta^{13}C_{cc}$ and Sr isotopes.

Fluid inclusions were examined in doubly-polished thick section (100 μm) slides, using a Nikon Eclipse E400 POL microscope. The isotope composition of fluid inclusion water was measured at the University of Innsbruck using a Delta V Advantage IRMS coupled to a Thermal Combustion/Elemental Analyser and a ConFlow II interface (Thermo Fisher) using the line, crusher and cryo-focussing cell described in Dublyansky and Spötl (2009). Samples were cut with a diamond band saw along visible petrographic boundaries in the speleothem, and therefore represent specific growth increments. Samples were analysed at least in duplicate, with the standard sampling protocol used on the Innsbruck instrument (Dublyansky and Spötl, 2009). To exclude the possibility of post-depositional diagenetic alteration, petrographic thin sections were investigated using transmitted-light microscopy. Results are detailed in Supplemental Information 1.

Optical emission spectroscopy (OES) was used to measure a variety of elemental concentrations, including Sr, along the main growth axis of SC-06-01. The low spatial resolution of trace elemental analyses (every 10 mm) does not allow to investigate time series of elemental variation but was useful to assess Sr contents of the samples for Sr isotope measurements by thermal ionisation mass spectrometry (TIMS). The samples for TIMS analyses were drilled using a hand held micro drill with a tungsten carbide drill bit. Sample sizes range between 2 and 4 mg, thus we achieved a minimum Sr load of 100 ng on the Re filaments for TIMS. Chemical sample preparation and subsequent TIMS measurement were done following standard protocols (Charlier et al., 2006). No spike was added to the samples prior to chemical purification. The Sr isotope measurements were done on a Triton TIMS housed at the Bristol Isotope Group laboratory, University of Bristol.

Results

Fluid inclusions

Petrographic analysis of the thick sections indicates that the distribution of fluid inclusions is highly variable, with macroscopically opaque "milky" calcite typical of rapidly growing intervals containing sometimes very abundant inclusions and the discoloured, translucent calcite of the slowly growing intervals being almost inclusion-free (Fig. 2). In most samples, two distinct populations of inclusions were identified with numerous small intra-crystalline inclusions and larger, but less frequent, inter-crystalline inclusions. Consequently, the volume of water analysed per sample was very variable (Fig. 3). Indeed, a significant proportion of individual fluid inclusion measurements had analyte volumes too small (<0.1 μL) to have confidence in the isotope results. A small number of analyses failed due to excessive water saturating the detector, and these have not been included in the datasets presented here. The major impact of the highly variable availability of inclusions in the speleothem is a significant bias in the analyses towards the most rapidly growing, and therefore probably humid, time periods. Three rapidly-growing phases are reported in SC-06-01, named Phase I (62-67ka), Phase II (53-50 ka) and Phase III (37-33 ka) (Hoffmann et al., 2016). Fluid inclusions for Phases I and II are isotopically similar (with $\delta^{18}O_{FI}$ ranging from -7.5 ‰ to -3.8 ‰ and from -8.5 ‰ to -3.2‰ respectively and $\delta^{2}H_{FI}$ ranging from -26.7 ‰ to -18.6 ‰ and from -29.4 ‰ to -16.1 ‰ respectively). However, compositions for Phase II are different, particularly with respect to deuterium ($\delta^{18}O_{FI}$ ranging from -8.9 ‰ to -4.5 ‰ and $\delta^{2}H_{FI}$ ranging from -38.3 ‰ to -25.1 ‰).

In most samples, achieving within-error replication ($\delta^{2}H$ ±1.5‰, $\delta^{18}O$: ±0.5‰) of both $\delta^{18}O_{fi}$ and $\delta^{2}H_{fi}$ was difficult. This must reflect more than one population of inclusions with different properties being present within at least some samples, and each replicate analysis represents some proportion of mixing between these populations. This suggests significant short-term variability in the composition of the water stored in the presumably rather small soil/epikarst zone overlying the cave. Consequently, any given time interval risks being under-sampled with regard to variability at that time. Although there is some visual correspondence between the $\delta^{18}O_{fi}$, $\delta^{2}H_{fi}$ and $\delta^{18}O_{cc}$ data series

(Fig. 4), it seems that the fluid inclusion time series risks aliasing changes seen in the calcite isotope time series. Consequently, the usefulness of interpretation that can be drawn from the episodic SC-01-06 fluid inclusion dataset when arranged as a time series is limited and we therefore largely focus our discussion to the properties of the population of waters as a full dataset. This approach minimises the impact the different populations can have on interpretation.

Figure 5 shows the SC-06-01 fluid inclusion dataset alongside Global Network of Isotopes in Precipitation (GNIP) datasets from Tunis World Meteorological Office (WMO station 6071500), Sfax (6075000) and Bet Dagan (4017900) (locations in Fig. 1) and other published precipitation datasets. The Tunisian datasets fit within a trend typical of the Global Meteoric Water Line (GMWL) ($\delta^2H = 8\delta^{18}O + 10$). However, all this data lies along a single moisture evolution trend, and the Tunis and Sfax populations overlap. The data from Bet Dagan exhibits a trend which is extremely close to being parallel to the global trend dominating in Tunisia, but translated by +10 ‰ in δ^2H, reflecting greater deuterium excess. This is typical of the Mediterranean Meteoric Water Line (MMWL) (Ayalon et al., 1998;Gat et al., 2003), and reflects internal recycling of water with consequent deuterium enrichment in the eastern Mediterranean and its bordering continental areas.

The values of δ^2H_{fi} and $\delta^{18}O_{fi}$ fit within the range of values for modern precipitation, giving confidence that these measurements do reflect past precipitation composition despite the influence of multiple inclusion populations. The lack of apparent scatter towards positive $\delta^{18}O$ values both in the precipitation and fluid inclusion datasets further indicates that the data represent little-altered precipitation values, and that surface re-evaporation was minor at least during humid phases. However, the range of fluid inclusion values is inconsistent with either an exclusively Tunis-type or an exclusively Bet Dagan-type moisture source for precipitation in Cyrenaica during MIS 3. Even when all but the subset of fluid inclusion analyses who replicates are similar are excluded (Fig. 6), the population is split between the Tunisian and Israeli precipitation end-members.

Strontium isotopes

The $^{87}Sr/^{86}Sr$ signal in the SC-06-01 record is rather invariable (Fig. 7), with all analyses indicating values within analytical error. Mean values vary between 0.708275 and 0.708524 and although there is an apparent trend from maxima at 34 and 64 ka BP with a minimum at 52 ka BP, which mimics the precession history, this is too weak to be significant relative to the error.

Calcite carbon isotopes

Both $\delta^{13}C_{cc}$ and $\delta^{18}O_{cc}$ show similar trends throughout the record (Fig. 8), indicating that depleted oxygen isotopes coincide with depleted carbon isotope values. This does not appear to arise from fractionation on the speleothem surface (Hoffmann et al., 2016), and so represents changes in soil bioproductivity acting in concert with changes in precipitation.

Discussion

Moisture advection during Libyan humid phases

The range of values of both individual and replicated fluid inclusion measurements can only be reconciled with multiple moisture sources. Most of the fluid inclusion data cluster between the weighted mean value for precipitation collected at Sfax with a mixed source from the Atlantic and western Mediterranean, ("Sfax Mixed" $\delta^{18}O_{ppt}$ = -4.93 ‰, $\delta^{2}H_{ppt}$ = -26 ‰; Fig. 9) and High Precipitation events at Bet Dagan ($\delta^{18}O_{ppt}$ = -6.33 ‰, $\delta^{2}H_{ppt}$ = -21.46 ‰; Fig. 9). However, the fluid inclusion data cluster also extends to the end member reflecting pure western Mediterranean sources at Sfax ($\delta^{18}O_{ppt}$ = -3.99 ‰, $\delta^{2}H_{ppt}$ = -20.3 ‰; Fig. 9), indicating a third end member composition with higher $\delta^{18}O_{ppt}$. The weighted mean value for Atlantic-sourced precipitation events in Sfax ($\delta^{18}O_{ppt}$ = -6.7 ‰, $\delta^{2}H_{ppt}$ = -37.7 ‰) is distant from any observed fluid inclusion value (Fig. 9). A simple 3-end-member unmixing of fluid inclusion isotope values using the quantitative approach of (Rogerson et al., 2011) indicates that Atlantic-sourced water supplied no more than 15 % of the mass for any given fluid inclusion analysis. However, the coherence of fluid inclusion isotope ratios with the weighted mean of "mixed" Atlantic and Mediterranean precipitation at Sfax suggests that this small Atlantic

influence is nevertheless persistent, and this must reflect synoptic westerly storms (Celle-Jeanton et al., 2001).

The simplest interpretation of the Susah Cave fluid inclusion data is therefore that they reflect a dynamic balance of moisture sources contributing to rainfall in Cyrenaica which resembles modern precipitation in Tunisia and Israel in roughly equal proportions. An alternative way to explain the trend of some points towards enriched $\delta^{18}O$ values on the GMWL would be the temperature-dependent fractionation that would be caused by a shift to summertime precipitation. We do not favour this explanation, as it requires a more fundamental reorganisation of regional atmospheric circulation than our suggestion that the winter storms observed today penetrated further east in the past.

Although the isotopic composition of Mediterranean water will have been more enriched during MIS 3 due to ice-volume effects and increased Mediterranean water residence time (Rohling and Bryden, 1994), the similar mean values of the SC-06-01 fluid inclusion waters compared to modern precipitation indicates the meteoric waterline at this time was not displaced to more enriched isotope values. This could reflect balancing of source water effects by changes in kinetic fractionation during evaporation (Goldsmith et al., 2017), which is controlled by normalised relative humidity. This would imply that the Mediterranean air masses were less saturated with moisture than today during MIS 3, which is consistent with the high deuterium excess $\delta^{2}H_{excess}$ values found in some fluid inclusion samples (Fig. 10), but is difficult to reconcile with the increased precipitation recorded in SC-06-01. In addition, changes in cloud height and cloud formation processes could possibly alter the isotopic fractionation in the atmosphere. Alternatively, the source water effect may be countered by increased runoff from the margins of the Mediterranean supplying isotopically depleted water to evaporating surface water. Isotopic "residuals" consistent with this argument are identified throughout MIS 3 in the eastern Mediterranean marine core LC21 (Grant et al., 2016), and this is also consistent with higher rainfall in Cyrenaica. We therefore favour the latter explanation.

Although we find that our results likely reflect patterns of atmospheric transport in MIS 3 comparable to today, it is possible that some moisture was drawn from re-evaporation of monsoon rain falling

301 further south, with no modern analogue in the region (Aggarwal et al., 2016). This water would likely
302 be extremely isotopically light, reflecting both monsoon-type compositions and further fractionation
303 during secondary evaporation. Moreover, a shift to more southerly-sourced regions is inconsistent
304 with Sr-isotope data from Susah Cave. Sr-isotopes are known to be sensitive to changes in transport of
305 Saharan dust (Frumkin and Stein, 2004), but even considering the most slowly-growing and most
306 rapidly-growing parts of SC-06-01, no significant difference in $^{87}Sr/^{86}Sr$ has been identified. Although
307 at times of extreme rainfall in the region, Saharan/Sahellian dust production is suppressed, this is not
308 true during MIS 3 (Collins et al., 2013). It seems that despite changes in the intensity of moisture
309 transport during the period 65-30 ka BP, there is no large-scale change in atmospheric dust transport
310 direction. This further supports our conclusion from the fluid inclusions that the Eastern
311 Mediterranean rainfall operating during precession parameter minima reflects enhanced internal
312 convection rather than transport of moisture from the east or south with an atmospheric circulation
313 pattern that prevails today.

314 Different sources at different times?

315 Phase II fluid inclusions are exceptional, because none show compositions consistent with a Bet
316 Dagan source. This is most clearly reflected in the δ^2H_{excess} values (Fig. 10), which show consistently
317 low values across Phase II comparing well to the Western water end-member (~10 ‰) and not the
318 Eastern water end-member (~30 ‰.). The lack of Eastern water during Phase II seems to reflect a
319 fundamental difference between this period and Phases I and III, as during this time all precipitation
320 was drawn from synoptic westerly storms in the winter. Consequently, it would seem that during the
321 obliquity-forced period of humidity, the Israeli-mode precipitation did not occur in the manner that it
322 did during both precession-forced periods of humidity. This difference in the origin of the moisture
323 feeding rainfall may explain the difference in average $\delta^{18}O_{cc}$ during these different phases (Hoffmann
324 et al., 2016), and why during some periods in Susah Cave show strong correlation with North Atlantic
325 temperature, whereas others do not (Hoffmann et al., 2016).

Palaeoclimatological significance

Most of the precipitation supplied to Cyrenaica during MIS 3 was sourced from within the Mediterranean basin, which exhibited a similar meteoric water cycle to that observed today, albeit with more freshwater influence. This is a critical observation, as the precipitation feeding runoff must be externally sourced if it is to materially change Mediterranean functioning, as is observed during sapropel events (Rohling et al., 2015). The internally-cycled water we report from Susah Cave cannot alter the basin-scale hydrological balance, and therefore is a minor influence on deep convection in the Mediterranean Sea (Bethoux and Gentili, 1999): put simply, this means evidence of increased rainfall in the coastal Mediterranean does not provide evidence for decreased net evaporation in the marine system. This observation is critical, as it decouples the processes of precipitation on the Mediterranean margins with sapropel formation, and consequent changes in momentum transfer to the North Atlantic (Rogerson et al., 2012).

Despite the low level of Atlantic moisture contributing to rainfall in Libya in MIS 3, the Western-sourced moisture is transported ~1500 km eastwards to reach Cyrenaica, which must reflect the mid-latitude storm track (Brayshaw et al., 2009). Consequently, although it does not seem that Atlantic moisture is important to the climatology of Cyrenaica, the momentum derived from Atlantic winter storms predicted by regional climate modelling (Brayshaw et al., 2009) and observed on the northern Mediterranean margin (Toucanne et al., 2015) remains pivotal to supplying moisture to North Africa. Consequently, the North Atlantic heat budget provides an important control on northern African rainfall in the past. In contrast, this control cannot explain changes in the Eastern-sourced rainfall revealed by our analysis. Eastern-sourced rainfall may occasionally relate to wintertime storms, as today (Gat et al., 2003), but essentially reflects convective rainfall with relatively small advection distances. It is likely this arises due to greater atmospheric convergence due to northward displacement of the annual average position of the ITCZ (Tuenter et al., 2003).

Palaeoclimatologically, our analysis reveals that 1) during northern hemisphere insolation peaks reflecting precession, coastal Libya experiences greater westerly advection of water due to an increase in Atlantic heat and greater convective rainfall due to migration of the ITCZ, whereas 2) insolation

peaks reflecting obliquity show increased Atlantic heat and westerlies, but no comparable change in the ITCZ position.

Implications for Susah Cave $\delta^{18}O_{cc}$

Aside from those data with high deuterium excess, which reflect influence from the Eastern Mediterranean source, much of the variance in the fluid inclusion dataset is captured by a two end-member mixing system resembling modern rainfall in Tunisia. One end-member is the Western Mediterranean source of Celle-Jeanton et al. (2001), but the other is isotopically too heavy to be identified with the Atlantic source. Rather, it resembles the "Sfax Mixed" population defined by Celle-Jeanton et al. (2001), reflecting a mixed source of moisture from both the Western Mediterranean and Atlantic. Consequently, although quantitatively minor amounts of Atlantic water reached the site, changes in the moisture advection driven by westerly winds had a strong influence on $\delta^{18}O_{dripwater}$ trends in time. At Sfax today, this influence causes a prominent bimodal behaviour with two rainfall maxima with different $\delta^{18}O_{ppt}$, which eliminates a simple and quantitative rainfall amount control on precipitation, which can be observed at Tunis (WMO code 6071500, https://nucleus.iaea.org/wiser/gnip.php). Furthermore, addition of heavy rain events derived from the Eastern Mediterranean aliases the tendency towards depleted $\delta^{18}O_{dripwater}$, as this water is also more depleted than modern Western Mediterranean precipitation. In the Bet Dagan data, there is also a tendency to lower $\delta^{18}O_{ppt}$ with higher precipitation amount, but the relationship between rainfall amount and rainfall isotope composition is not identical to Tunis. Ultimately, it seems likely that rainfall amount changes at Susah Cave do cause depleted (enriched) $\delta^{18}O_{cc}$ values to be associated with high (low) rainfall, but this is too complicated by independent changes increases (decreases) in westerly moisture advection and increases (decreases) in convergence. Qualitatively, all these parameters are expected symptoms of North African humid phases and so these trends remain a valuable expression of climatic variability. Quantitatively, more information is required to translate the trends into fully-functional palaeoclimatologies, and this analysis pivots on whether $\delta^{18}O_{cc}$ trends reflect changes in water deficit / surplus in Cyrenaica.

Although it is likely the oxygen isotope fractionation during calcite precipitation occurred close to isotope equilibrium (Hoffmann et al., 2016), there is a good degree of correspondence between positive and negative phases in $\delta^{18}O_{cc}$ and $\delta^{13}C_{cc}$, indicating a shared control. Indeed, $\delta^{13}C_{cc}$ has a markedly higher amplitude variability than $\delta^{18}O_{cc}$. More isotopically depleted carbon may represent increased incorporation of respired soil carbon, increased dominance of C3 over C4 plants, and/or decreased degassing of aquifer water (Baker et al., 1997). Today, the Susah Cave location on Jebel Malh has very thin soil cover, colonised by shrubby maquis vegetation. Soil respiration and colonisation by C3 plants is limited by the strong water deficit of the region, and aquifer water outgassing is enhanced by long residence times due to low water infiltration. Increased water availability will progressively deplete the $\delta^{13}C$ of dripwater by all three mechanisms described above. Consequently, all three of these processes promote correlation between $\delta^{13}C_{cc}$ and precipitation amount. Within the $\delta^{18}O_{cc}$ data series, peak growth rates occur both during relatively enriched and relatively depleted isotope stages. This is not the case for $\delta^{13}C_{cc}$, which more consistently shows depleted values during times of rapid growth (SC-06-01 growth phases shown in Fig. 11). We therefore consider it likely that $\delta^{13}C_{cc}$ indeed more accurately records rainfall amount than $\delta^{18}O_{cc}$ does.

Conclusions and Implications

A key feature of this combined dataset is the long-term sinusoidal trend in both the $\delta^{18}O_{cc}$ and $\delta^{2}H_{fi}$, reflecting the differing rainfall regimes dominant between Humid Phases I and III compared to Phase II. This is not developed in $\delta^{13}C_{cc,}$ implying that the process forcing the long-term cycle in moisture source is not impacting on carbon dynamics in the soil and epikarst. We therefore conclude that there is a mixed amount and source control on $\delta^{18}O$ and $\delta^{2}H$ in the SC-01-06 record, whereas $\delta^{13}C$ is dominantly controlled by water availability.

The fluid inclusions from SC-06-01 show that rainfall compositions in the southeast Mediterranean region during MIS 3 were comparable to modern rainfall compositions recorded in regional GNIP datasets. However, the diversity of compositions is impossible to explain with a single rainfall source, rather indicating that moisture derived from the Atlantic, the Western Mediterranean and the Eastern

Mediterranean basins have all contributed to MIS 3 precipitation in Libya. This requires both enhanced westerly advection of moisture to this region, reflecting the Atlantic storm track, and enhanced convective rainfall within the Eastern Mediterranean basin. There is some indication that these two mechanisms differ in terms of their response to orbital forcing, with precession parameter minima enhancing westerly advection and internal convection, whereas obliquity minima enhance westerly advection without significantly altering internal convection.

Crucially, this picture is most consistent with atmospheric circulation over the Mediterranean remaining essentially unchanged during precession cycles. This is consistent with regional climate model experiments showing major enhancement of winter westerly storm activity, but it not consistent with the extreme migration of the ITCZ, where the monsoon belt approaches the North African coast. The strong implication is that a significant arid belt is retained between the Mediterranean and the ITCZ, even when northernmost Africa is experiencing significantly enhanced rainfall.

It is likely that rainfall amount played a role in controlling the isotopic composition of the calcite in this speleothem ($\delta^{18}O_{cc}$). However, the more depleted values reflecting higher rainfall are also consistent with different mixing between the end members identified by the fluid inclusion analysis. The structure of the $\delta^{13}C_{cc}$ record provides an independent means of assessing changes in water surplus / deficit, as more depleted values will reflect lower aquifer residence times, enhanced soil respiration and changes in vegetation structure, all of which are limited by water availability in this semi-arid environment. Combined analysis of the proxies provides a powerful new demonstration that the northeast Libyan climate was more humid during millennial-scale warm periods in the North Atlantic realm, but quantification will be dependent on generating unambiguous independent evidence for water availability in the soil and epikarst.

Acknowledgements

We thank the Royal Geographical Society for the pump-priming investment that began this work (Thesiger-Oman International Fellowship 2009), the Natural Environment Research Council for

providing the funds that made the analytical work on this project possible (NE/J014133/1) and The Leverhulme Trust for funding activities within the associated International Network (IN-2012-113). We also thank two anonymous reviewers for considerably improving the quality and accessibility of this paper.

References

Arienzo, M.M. et al. 2015. Bahamian speleothem reveals temperature decrease associated with Heinrich stadials. EPSL 430, 377-386.

Adkins, J., Demenocal, P., and Eshel, G.: The "African humid period" and the record of marine upwelling from excess 230Th in Ocean Drilling Program Hole 658C, Paleoceanography and Paleoclimatology, 21, 2006.

Aggarwal, P. K., Romatschke, U., Araguas-Araguas, L., Belachew, D., Longstaffe, F. J., Berg, P., Schumacher, C., and Funk, A.: Proportions of convective and stratiform precipitation revealed in water isotope ratios, Nat. Geosci., 9, 624, 2016.

Ait Brahim, Y., Cheng, H., Sifeddine, A., Wassenburg, J. A., Cruz, F. W., Khodri, M., Sha, L., Pérez-Zanón, N., Beraaouz, E. H., Apaéstegui, J., Guyot, J.-L., Jochum, K. P., and Bouchaou, L.: Speleothem records decadal to multidecadal hydroclimate variations in southwestern Morocco during the last millennium, Earth and Planetary Science Letters, 476, 1-10, https://doi.org/10.1016/j.epsl.2017.07.045, 2017.

Arienzo, M. M., Swart, P. K., Pourmand, A., Broad, K., Clement, A. C., Murphy, L. N., Vonhof, H. B., and Kakuk, B.: Bahamian speleothem reveals temperature decrease associated with Heinrich stadials, Earth and Planetary Science Letters, 430, 377-386, 2015.

Armitage, S. J., Drake, N. A., Stokes, S., El-Hawat, A., Salem, M., White, K., Turner, P., and McLaren, S. J.: Multiple phases of north African humidity recorded in lacustrine sediments from the fazzan basin, Libyan sahara, Quaternary Geochronology, 2, 181-186, 2007.

Ayalon, A., Bar-Matthews, M., and Sass, E.: Rainfall-recharge relationships within a karstic terrain in the Eastern Mediterranean semi-arid region, Israel: δ18O and δD characteristics, Journal of Hydrology, 207, 18-31, 10.1016/S0022-1694(98)00119-X, 1998.

Baker, A., Ito, E., Smart, P. L., and McEwan, R. F.: Elevated and variable values of 13C in speleothems in a British cave system, Chemical Geology, 136, 263-270, 1997.

Ballais, J.-L.: Evolution holocène de la Tunisie saharienne et présaharienne, Méditerranée, 74, 31-38, 1991.

Bethoux, J. P., and Gentili, B.: Functioning of the Mediterranean Sea: past and present changes related to freshwater input and climate changes, Journal of Marine Systems, 20, 33-47, 1999.

Black, E., Brayshaw, D. J., and Rambeau, C. M. C.: Past, present and future precipitation in the Middle East: Insights from models and observations, Philosophical Transactions of the Royal Society A: Mathematical, Physical and Engineering Sciences, 368, 5173-5184, 10.1098/rsta.2010.0199, 2010.

Bosmans, J. H. C., Drijfhout, S. S., Tuenter, E., Hilgen, F. J., Lourens, L. J., and Rohling, E. J.: Precession and obliquity forcing of the freshwater budget over the Mediterranean, Quaternary Science Reviews, 123, 16-30, 10.1016/j.quascirev.2015.06.008, 2015.

Brayshaw, D. J., Woollings, T., and Vellinga, M.: Tropical and Extratropical Responses of the North Atlantic Atmospheric Circulation to a Sustained Weakening of the MOC, Journal of Climate, 22, 3146-3155, 10.1175/2008jcli2594.1, 2009.

Brun, A.: Reflections on the pluvial and arid periods of the Upper Pleistocene and of the Holocene in Tunisia, Palaeoecology of Africa and the surrounding islands. Vol. 22. Proc. symposium on African palynology, Rabat, 1989, 157-170, 1991.

476 Cancellieri E., Cremaschi M., Zerboni A., and S., d. L.: Climate, Environment, and Population
477 Dynamics in Pleistocene Sahara, in: Africa from MIS 6-2. Vertebrate Paleobiology and
478 Paleoanthropology. , edited by: Jones S., and B., S., Springer, Dordrecht, 2016.
479 Celle-Jeanton, H., Zouari, K., Travi, Y., and Daoud, A.: Caractérisation isotopique des pluies en
480 Tunisie. Essai de typologie dans la région de Sfax, Sciences de la Terre et des planètes, 333, 625-631,
481 2001.
482 Charlier, B., Ginibre, C., Morgan, D., Nowell, G., Pearson, D., Davidson, J., and Ottley, C.: Methods for
483 the microsampling and high-precision analysis of strontium and rubidium isotopes at single crystal
484 scale for petrological and geochronological applications, Chemical Geology, 232, 114-133, 2006.
485 Collins, J. A., Govin, A., Mulitza, S., Heslop, D., Zabel, M., Hartmann, J., Röhl, U., and Wefer, G.:
486 Abrupt shifts of the Sahara–Sahel boundary during Heinrich stadials, Climate of the Past, 9, 1181-
487 1191, 2013.
488 Collins, J. A., Prange, M., Caley, T., Gimeno, L., Beckmann, B., Mulitza, S., Skonieczny, C., Roche, D.,
489 and Schefuß, E.: Rapid termination of the African humid period triggered by northern high-latitude
490 cooling, Nature Communications, 8, 1372, 2017.
491 Dayan, U., Nissen, K., and Ulbrich, U.: Review Article: Atmospheric conditions inducing extreme
492 precipitation over the eastern and western Mediterranean, Nat. Hazards Earth Syst. Sci., 15, 2525-
493 2544, 10.5194/nhess-15-2525-2015, 2015.
494 deMenocal, P., Ortiz, J., Guilderson, T., Adkins, J., Sarnthein, M., Baker, L., and Yarusinsky, M.: Abrupt
495 onset and termination of the African Humid Period: rapid climate responses to gradual insolation
496 forcing. , Quaternary Science Reviews, 19, 347- 361, 2000.
497 Drake, N. A., El-Hawat, A. S., Turner, P., Armitage, S. J., Salem, M. J., White, K. H., and McLaren, S.:
498 Palaeohydrology of the Fazzan Basin and surrounding regions: The last 7 million years,
499 Palaeogeography Palaeoclimatology Palaeoecology, 263, 131-145, 10.1016/j.palaeo.2008.02.005,
500 2008.
501 Drake, N. A., Blench, R. M., Armitage, S. J., Bristow, C. S., and White, K. H.: Ancient watercourses and
502 biogeography of the Sahara explain the peopling of the desert, Proc. Natl. Acad. Sci. U. S. A., 108,
503 458-462, 10.1073/pnas.1012231108, 2011.
504 Dublyansky, Y. V., and Spötl, C.: Hydrogen and oxygen isotopes of water from inclusions in minerals:
505 Design of a new crushing system and on-line continous-flow isotope ratio mass spectrometric
506 analysis, Rapid Communications in Mass Spectrometry, 23, 2605-2613, 10.1002/rcm.4155, 2009.
507 Fleitmann, D., Burns, S. J., Neff, U., Mangini, A., and Matter, A.: Changing moisture sources over the
508 last 330,000 years in Northern Oman from fluid-inclusion evidence in speleothems, Quaternary
509 Research, 60, 223-232, http://dx.doi.org/10.1016/S0033-5894(03)00086-3, 2003.
510 Fontes, J. C., and Gasse, F.: PALHYDAF (Palaeohydrology in Africa) program: objectives, methods,
511 major results, Palaeogeography, Palaeoclimatology, Palaeoecology, 84, 191-215, 10.1016/0031-
512 0182(91)90044-R, 1991.
513 Frumkin, A., and Stein, M.: The Sahara-East Mediterranean dust and climate connection revealed by
514 strontium and uranium isotopes in a Jerusalem speleothem, Earth and Planetary Science Letters,
515 217, 451-464, 10.1016/s0012-821x(03)00589-2, 2004.
516 Gasse, F., and Campo, E. v.: Abrupt post-glacial climate events in west Asia and north Africa
517 monsoon domains, Earth and Planetary Science Letters, 126, 435-456, 1994.
518 Gasse, F.: Diatom-inferred salinity and carbonate oxygen isotopes in Holocene waterbodies of the
519 western Sahara and Sahel (Africa), Quaternary Science Reviews, 21, 737-767, 2002.
520 Gat, J. R., Klein, B., Kushnir, Y., Roether, W., Wernli, H., Yam, R., and Shemesh, A.: Isotope
521 composition of air moisture over the Mediterranean Sea: An index of the air-sea interaction pattern,
522 Tellus, Series B: Chemical and Physical Meteorology, 55, 953-965, 10.1034/j.1600-
523 0889.2003.00081.x, 2003.
524 Genty, D., Blamart, D., Ghaleb, B., Plagnes, V., Causse, C., Bakalowicz, M., Zouari, K., Chkir, N.,
525 Hellstrom, J., Wainer, K., and Bourges, F.: Timing and dynamics of the last deglaciation from

526 European and North African δ13C stalagmite profiles-comparison with Chinese and South
527 Hemisphere stalagmites, Quaternary Science Reviews, 25, 2118-2142, 2006.
528 Goldsmith, Y., Polissar, P. J., Ayalon, A., Bar-Matthews, M., deMenocal, P. B., and Broecker, W. S.:
529 The modern and Last Glacial Maximum hydrological cycles of the Eastern Mediterranean and the
530 Levant from a water isotope perspective, Earth and Planetary Science Letters, 457, 302-312,
531 http://dx.doi.org/10.1016/j.epsl.2016.10.017, 2017.
532 Grant, K. M., Grimm, R., Mikolajewicz, U., Marino, G., Ziegler, M., and Rohling, E. J.: The timing of
533 Mediterranean sapropel deposition relative to insolation, sea-level and African monsoon changes,
534 Quaternary Science Reviews, 140, 125-141, http://dx.doi.org/10.1016/j.quascirev.2016.03.026,
535 2016.
536 Harrison, S., Bartlein, P., Izumi, K., Li, G., Annan, J., Hargreaves, J., Braconnot, P., and Kageyama, M.:
537 Evaluation of CMIP5 palaeo-simulations to improve climate projections, Nature Climate Change, 5,
538 735-743, 2015.
539 Hoffmann, D. L., Rogerson, M., Spötl, C., Luetscher, M., Vance, D., Osborne, A. H., Fello, N. M., and
540 Moseley, G. E.: Timing and causes of North African wet phases during MIS 3 and implications for
541 Modern Human migration, Nature Scienfiic Reports, 6, 36367, 2016.
542 IPCC: Climate Change 2014: Impacts, Adaptation, and Vulnerability. Part B: Regional Aspects.
543 Contribution of Working Group II to the Fifth Assessment Report of the Intergovernmental Panel on
544 Climate Change, United Kingdom and New York, 688, 2014.
545 Jolly, D., Prentice, I. C., Bonnefille, R., Ballouche, A., Bengo, M., Brenac, P., Buchet, G., Burney, D.,
546 Cazet, J. P., Cheddadi, R., Edorh, T., Elenga, H., Elmoutaki, S., Guiot, J., Laarif, F., Lamb, H., Lezine, A.
547 M., Maley, J., Mbenza, M., Peyron, O., Reille, M., Reynaud-Farrera, I., Riollet, G., Ritchie, J. C., Roche,
548 E., Scott, L., Ssemmanda, I., Straka, H., Umer, M., Van Campo, E., Vilimumbalo, S., Vincens, A., and
549 Waller, M.: Biome reconstruction from pollen and plant macrofossil data for Africa and the Arabian
550 peninsula at 0 and 6000 years, Journal of Biogeography, 25, 1007-1027, 1998.
551 Langgut, D., Almogi-Labin, A., Bar-Matthews, M., Pickarski, N., and Weinstein-Evron, M.: Evidence
552 for a humid interval at ~56–44 ka in the Levant and its potential link to modern humans dispersal
553 out of Africa, Journal of Human Evolution, 124, 75-90, 10.1016/j.jhevol.2018.08.002, 2018.
554 McGarry, S., Bar-Matthews, M., Matthews, A., Vaks, A., Schilman, B., and Ayalon, A.: Constraints on
555 hydrological and paleotemperature variations in the Eastern Mediterranean region in the last 140 ka
556 given by the δD values of speleothem fluid inclusions, Quaternary Science Reviews, 23, 919-934,
557 http://dx.doi.org/10.1016/j.quascirev.2003.06.020, 2004.
558 Meckler, A. N., Affolter, S., Dublyansky, Y. V., Krüger, Y., Vogel, N., Bernasconi, S. M., Frenz, M.,
559 Kipfer, R., Leuenberger, M., Spötl, C., Carolin, S., Cobb, K. M., Moerman, J., Adkins, J. F., and
560 Fleitmann, D.: Glacial–interglacial temperature change in the tropical West Pacific: A comparison of
561 stalagmite-based paleo-thermometers, Quaternary Science Reviews, 127, 90-116,
562 http://dx.doi.org/10.1016/j.quascirev.2015.06.015, 2015.
563 Nicoll, K.: A revised chronology for Pleistocene paleolakes and Middle Stone Age – Middle Paleolithic
564 cultural activity at Bîr Tirfawi – Bîr Sahara in the Egyptian Sahara, Quaternary International, 463, 18-
565 28, https://doi.org/10.1016/j.quaint.2016.08.037, 2018.
566 Osborne, A., Vance, D., Rohling, E., Barton, N., Rogerson, M., and Fello, N.: A humid corridor across
567 the Sahara for the migration of early modern humans out of Africa 120,000 years ago, Proc. Natl.
568 Acad. Sci. U. S. A., doi_10.1073_pnas.0804472105, 2008.
569 Osborne, A. H., Marino, G., Vance, D., and Rohling, E. J.: Eastern Mediterranean surface water Nd
570 during Eemian sapropel S5: monitoring northerly (mid-latitude) versus southerly (sub-tropical)
571 freshwater contributions, Quaternary Science Reviews, 29, 2473-2483,
572 http://dx.doi.org/10.1016/j.quascirev.2010.05.015, 2010.
573 Pascale, S., Gregory, J. M., Ambaum, M., and Tailleux, R.: Climate entropy budget of the HadCM3
574 atmosphere-ocean general circulation model and of FAMOUS, its low-resolution version, Climate
575 Dynamics, 36, 1189-1206, 10.1007/s00382-009-0718-1, 2011.

Peleg, N., and Morin, E.: Convective rain cells: Radar-derived spatiotemporal characteristics and synoptic patterns over the eastern Mediterranean, J. Geophys. Res. D Atmos., 117, 10.1029/2011JD017353, 2012.
PETIT-MAIRE, N., BUROLLET, P. F., A BALLAIS, J.-L., A FONTUGNE, M., A ROSSO, J.-C., A LAZAAR, A., and Gauthier-Villars, I.: Paléoclimats holocènes du Sahara septentrional. Dépôts lacustres et terrasses alluviales en bordure du Grand Erg Oriental à l'extrême-Sud de la Tunisie, Comptes rendus de l'Académie des sciences. Série 2, Mécanique, Physique, Chimie, Sciences de l'univers, Sciences de la Terre 312, 1661-1666, 1991.
Peyron, O., Jolly, D., Braconnot, P., Bonnefille, R., Guiot, J., Wirrmann, D., and Chalie, F.: Quantitative reconstructions of annual rainfall in Africa 6000 years ago: Model-data comparison, Journal of Geophysical Research-Atmospheres, 111, D24110
Artn d24110, 2006.
Prentice, I. C., and Jolly, D.: Mid-Holocene and glacial-maximum vegetation geography of the northern continents and Africa, Journal of Biogeography, 27, 507-519, 2000.
Revel, M., Ducassou, E., Grousset, F. E., Bernasconi, S. M., Migeon, S., Revillon, S., Mascle, J., Murat, A., Zaragosi, S., and Bosch, D.: 100,000 Years of African monsoon variability recorded in sediments of the Nile margin, Quaternary Science Reviews, 29, 1342-1362, 10.1016/j.quascirev.2010.02.006, 2010.
Rogerson, M., Schönfeld, J., and Leng, M.: Qualitative and quantitative approaches in palaeohydrography: A case study from core-top parameters in the Gulf of Cadiz, Marine Geology, 280, 150-167, 2011.
Rogerson, M., Rohling, E. J., Bigg, G. R., and Ramirez, J.: Palaeoceanography of the Atlantic-Mediterranean Exchange: Overview and first quantitative assessment of climatic forcing. , Reviews of Geophysics, 50, DOI: 8755-1209/8712/2011RG000376, 2012.
Rohling, E., Marino, G., and Grant, K.: Mediterranean climate and oceanography, and the periodic development of anoxic events (sapropels), Earth-Science Reviews, 143, 62-97, 2015.
Rohling, E. J., and Bryden, H. L.: Estimating past changes in the Eastern Mediterranean freshwater budget, using reconstructions of sea level and hydrography, Proceedings Koninklijke Nederlandse Akademie van Wetenschappen, Serie B, 97, 201-217, 1994.
Rowan, J. S., Black, S., Macklin, M. G., Tabner, B. J., and Dore, J.: Quaternary environmental change in Cyrenaica evidenced by U-Th, ESR and OSL of coastal alluvial fan sequences. , Libyan Studies, 31, 5-16, 2000.
Schwarcz, H. P., Harmon, R. S., Thompson, P., and Ford, D. C.: Stable isotope studies of fluid inclusions in speleothems and their paleoclimatic significance, Geochimica et Cosmochimica Acta, 40, 657-665, http://dx.doi.org/10.1016/0016-7037(76)90111-3, 1976.
Smith, J. R., Giegengack, R., Schwarcz, H. P., McDonald, M. M. A., Kleindienst, M. R., Hawkins, A. L., and Churcher, C. S.: A reconstruction of quaternary pluvial environments and human occupations using stratigraphy and geochronology of fossil-spring tufas, Kharga Oasis, Egypt, Geoarchaeology-an International Journal, 19, 407-439, 2004.
Smith, J. R., Hawkins, A. L., Asmerom, Y., Polyak, V., and Giegengack, R.: New age constraints on the Middle Stone Age occupations of Kharga Oasis, Western Desert, Egypt, Journal of Human Evolution, 52, 690-701, 2007.
Swezey, C.: Eolian sediment responses to late Quaternary climate changes: temporal and spatial patterns in the Sahara, Palaeogeography, Palaeoclimatology, Palaeoecology, 167, 119-155, 2001.
Toucanne, S., Angue Minto'o, C. M., Fontanier, C., Bassetti, M.-A., Jorry, S. J., and Jouet, G.: Tracking rainfall in the northern Mediterranean borderlands during sapropel deposition, Quaternary Science Reviews, 129, 178-195, http://dx.doi.org/10.1016/j.quascirev.2015.10.016, 2015.
Tuenter, E., Weber, S. L., Hilgen, F. J., and Lourens, L. J.: The response of the African summer monsoon to remote and local forcing due to precession and obliquity, Global and Planetary Change, 36, 219-235, 2003.

626 Vaks, A., Woodhead, J., Bar-Matthews, M., Ayalon, A., Cliff, R., Zilberman, T., Matthews, A., and
627 Frumkin, A.: Pliocene–Pleistocene climate of the northern margin of Saharan–Arabian Desert
628 recorded in speleothems from the Negev Desert, Israel, Earth and Planetary Science Letters, 368, 88-
629 100, 2013.
630 Van Breukelen, M., Vonhof, H., Hellstrom, J., Wester, W., and Kroon, D.: Fossil dripwater in
631 stalagmites reveals Holocene temperature and rainfall variation in Amazonia, Earth and Planetary
632 Science Letters, 275, 54-60, 2008.
633 Wainer, K., Genty, D., Blamart, D., Daëron, M., Bar-Matthews, M., Vonhof, H., Dublyansky, Y., Pons-
634 Branchu, E., Thomas, L., van Calsteren, P., Quinif, Y., and Caillon, N.: Speleothem record of the last
635 180 ka in Villars cave (SW France): Investigation of a large δ18O shift between MIS6 and MIS5,
636 Quaternary Science Reviews, 30, 130-146, http://dx.doi.org/10.1016/j.quascirev.2010.07.004, 2011.
637 Wassenburg, J. A., Immenhauser, A., Richter, D. K., Niedermayr, A., Riechelmann, S., Fietzke, J.,
638 Scholz, D., Jochum, K. P., Fohlmeister, J., Schröder-Ritzrau, A., Sabaoui, A., Riechelmann, D. F. C.,
639 Schneider, L., and Esper, J.: Moroccan speleothem and tree ring records suggest a variable positive
640 state of the North Atlantic Oscillation during the Medieval Warm Period, Earth and Planetary Science
641 Letters, 375, 291-302, http://dx.doi.org/10.1016/j.epsl.2013.05.048, 2013.
642 Wassenburg, J. A., Dietrich, S., Fietzke, J., Fohlmeister, J., Jochum, K. P., Scholz, D., Richter, D. K.,
643 Sabaoui, A., Spötl, C., Lohmann, G., Andreae, Meinrat O., and Immenhauser, A.: Reorganization of
644 the North Atlantic Oscillation during early Holocene deglaciation, Nat. Geosci., 9, 602,
645 10.1038/ngeo2767

646 https://www.nature.com/articles/ngeo2767#supplementary-information, 2016.

647

648

649

650

651 Figure Captions

652 Figure 1: Map showing the location of Susah Cave (filled circle) and GNIP sites used in the discussion
653 (open circles). Blue stars indicate sources of marine water evaporation discussed in the text. Grey
654 arrows indicate recent average winter wind direction.

655 Figure 2) Macroscopic structure of SC-06-01 speleothem, showing alternation of transparent and
656 milky fabrics

657 Figure 3) Variability of water content (μL) per unit mass of speleothem (g) in SC-06-01 fluid inclusion
658 samples. Grey area shows working range of instrument.

659 Figure 4a) Fluid inclusion oxygen isotope values ($\delta^{18}O_{fi}$; black crosses) compared to calcite oxygen
660 isotope values ($\delta^{18}O_{cc}$; blue circles and line); 4b) Fluid inclusion hydrogen isotope values ($\delta^{2}H_{fi}$; black
661 crosses) compared to $\delta^{18}O_{cc}$ (blue circles and line). Growth Phases I, II and III are shown as grey
662 areas.

663 Figure 5a) Regional precipitation isotope data. Thick line represents Global Meteoric Water Line,
664 dashed thick line represents Mediterranean Meteoric Water Line and thin lines representing
665 expected range of deviation (±10 ‰ $\delta^{2}H_{ppt}$) below GMWL and above MMWL. Bet Dagan, Tunis and
666 Sfax GNIP datasets (http://www-naweb.iaea.org/napc/ih/IHS_resources_gnip.html). Sfax Atlantic

667 and Mediterranean Rainfall are taken from Celle-Jeanton et al. (2001). 5b-d) Summarised
668 precipitation isotopes, and fluid inclusion measurements for SC-06-01 for Phases I, II and II
669 respectively.

670 Figure 6) Double-replicated fluid inclusion measurements from SC-06-01, and regional precipitation
671 isotope trends.

672 Figure 7) $^{87}Sr/^{86}Sr$ record for SC-06-01, compared to calcite $\delta^{18}O_{cc}$ record (light grey line). Error bars
673 are 2σ. Growth Phases I, II and III are shown as grey areas.

674 Figure 8) Carbon isotope ($\delta^{13}C_{cc}$) record for SC-06-01 compared to oxygen isotope record ($\delta^{18}O_{cc}$;
675 (Hoffmann et al., 2016)). Growth Phases I, II and III are shown as grey areas.

676 Figure 9) Fluid inclusion measurements relative to summarised precipitation data and the modern
677 precipitation end members used in the discussion. Solid lines are the Meteoric Water Lines as in Fig.
678 5a. Precipitation and fluid inclusion measurements are as shown in Figure 5b. “Mean Atlantic”, “Sfax
679 Mixed”, “Sfax Med” and “High Precip Atlantic” indicate the mean of measurements in Celle-Jeanton
680 et al. (2001) originating from Atlantic moisture, mixed source, Mediterranean moisture and High
681 Precipitation measurements from an Atlantic moisture source (as described in Discussion)
682 respectively. “Mean Bet Dagan” is the mean of GNIP measurements from this location, and “High
683 Precip Bet Dagan” is the subset of high precipitation measurements as described in the Discussion.

684 Figure 10) Fluid inclusion deuterium excess ($\delta^2H_{excess\text{-}FI}$) relative to calcite $\delta^{18}O_{cc}$. Note some fluid
685 inclusions (70 to 60 ka BP and 40 to 30 ka BP) show high ($\delta^2H_{excess\text{-}Fi}$ indicative of an Eastern
686 Mediterranean source. Growth Phases I, II and III are shown as grey areas.

687

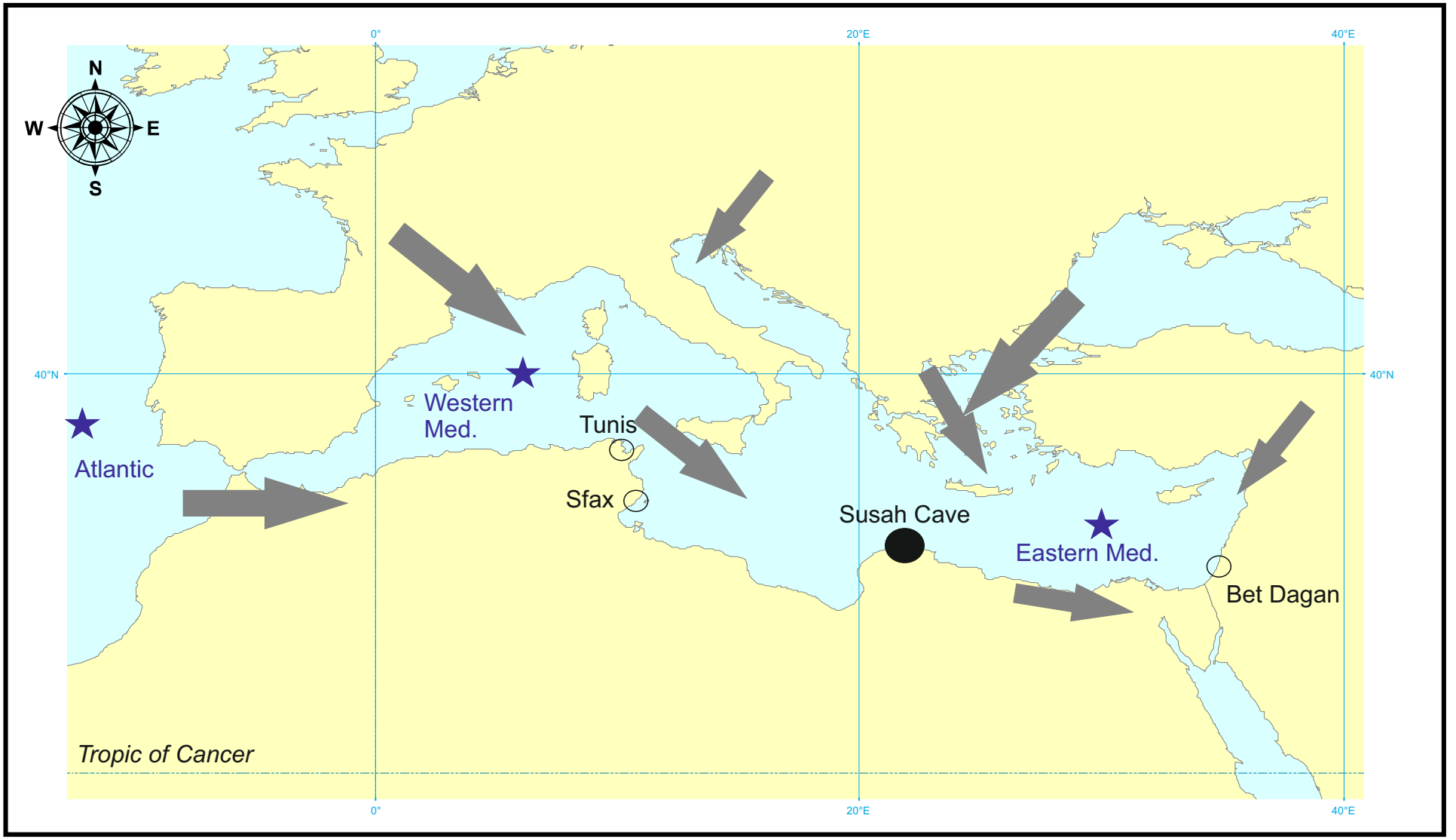
N
W
E
S
0°
20°E
40°E
40°N
Western
Med.
Tunis
Sfax
Atlantic
Susah Cave
Eastern Med.
Bet Dagan
Tropic of Cancer

Figure 2

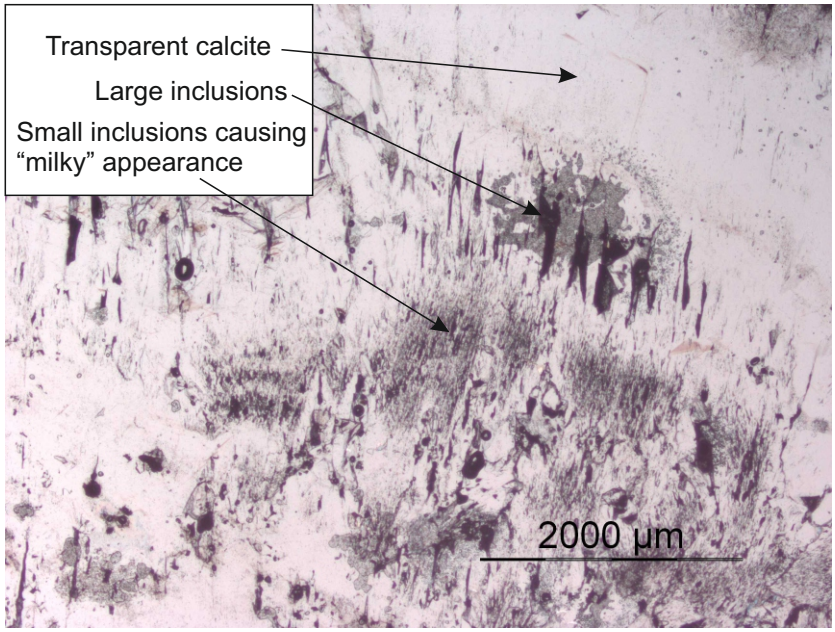
Transparent calcite
Large inclusions
Small inclusions causing "milky" appearance
2000 µm

Figure 3

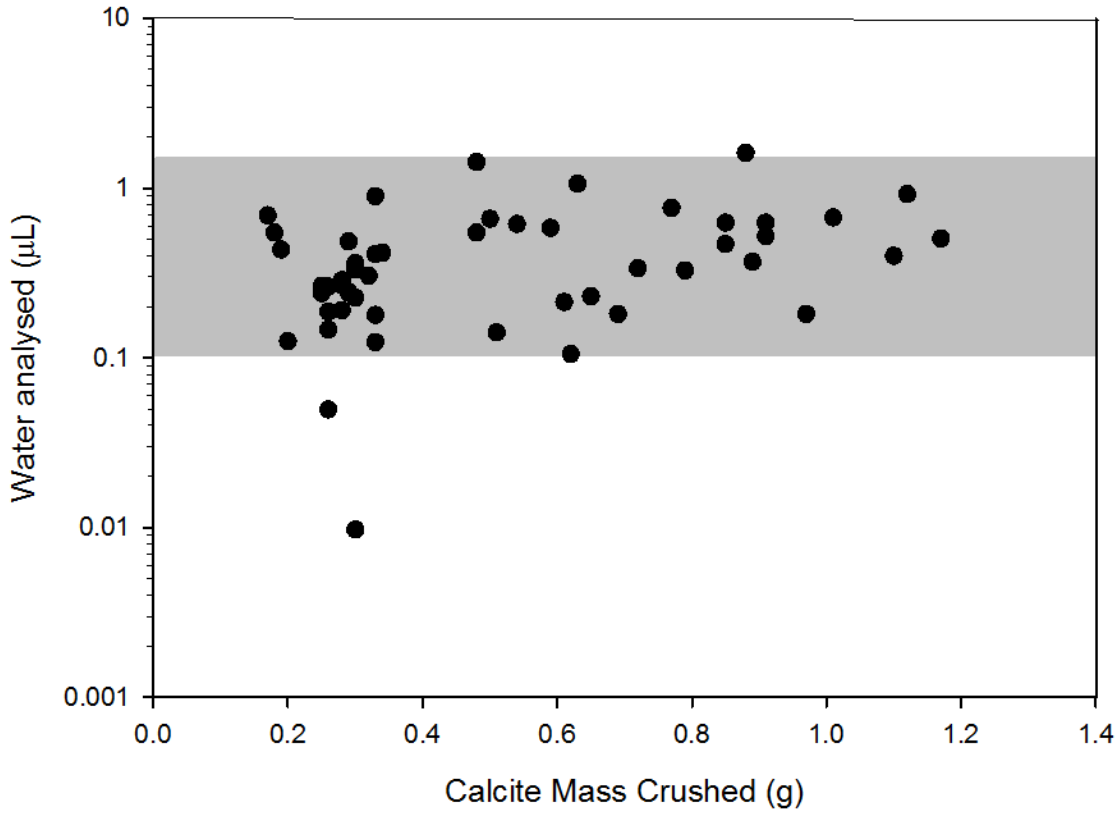
10
1
0.1
0.01
0.001
Water analysed (µL)
0.0
0.2
0.4
0.6
0.8
1.0
1.2
1.4
Calcite Mass Crushed (g)

Figure 4a

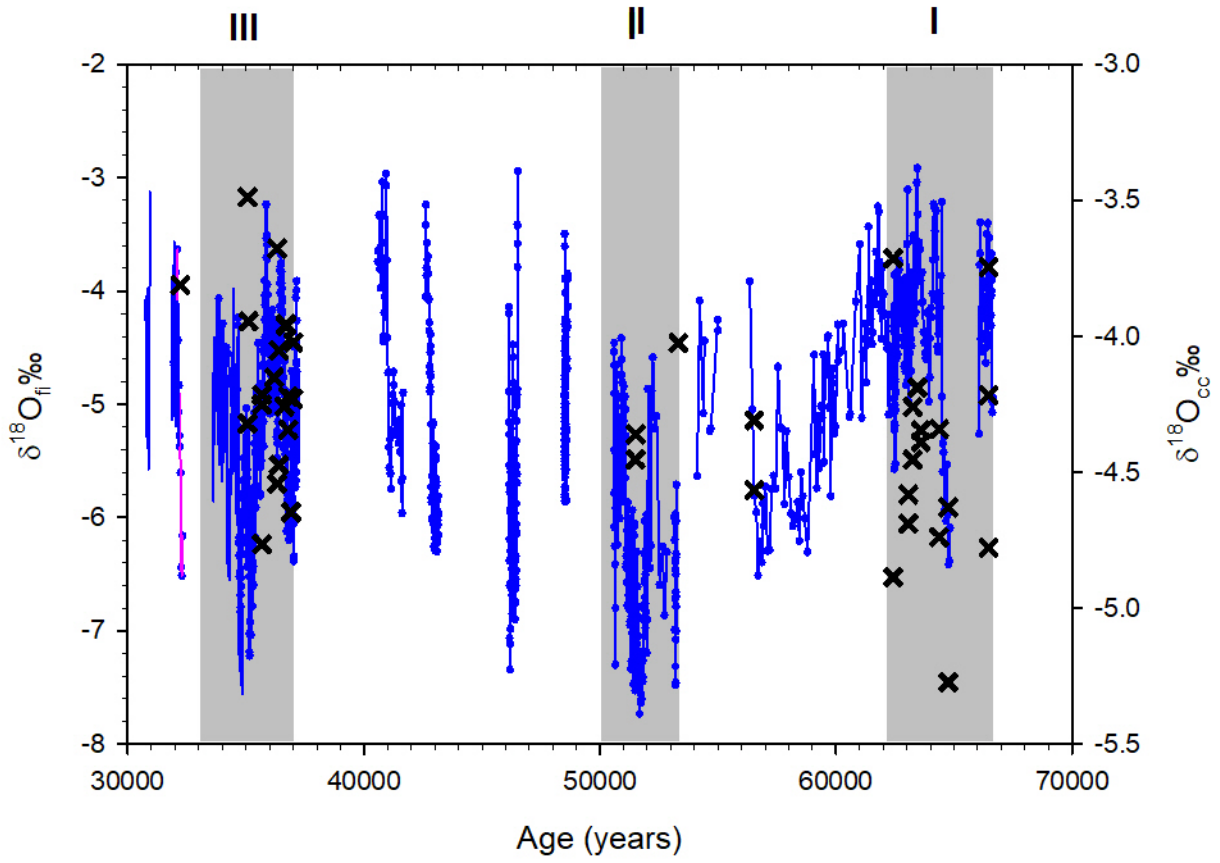

Figure 4b

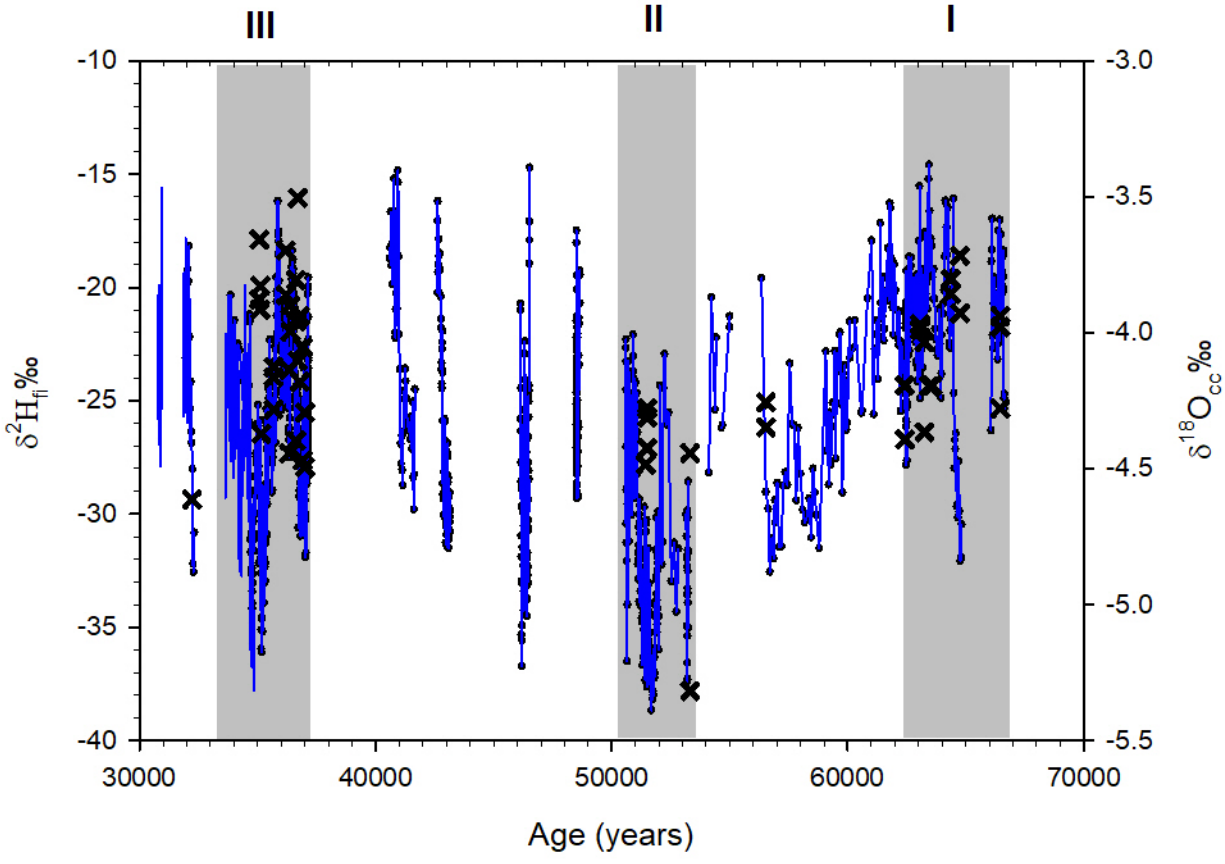

Figure 5a

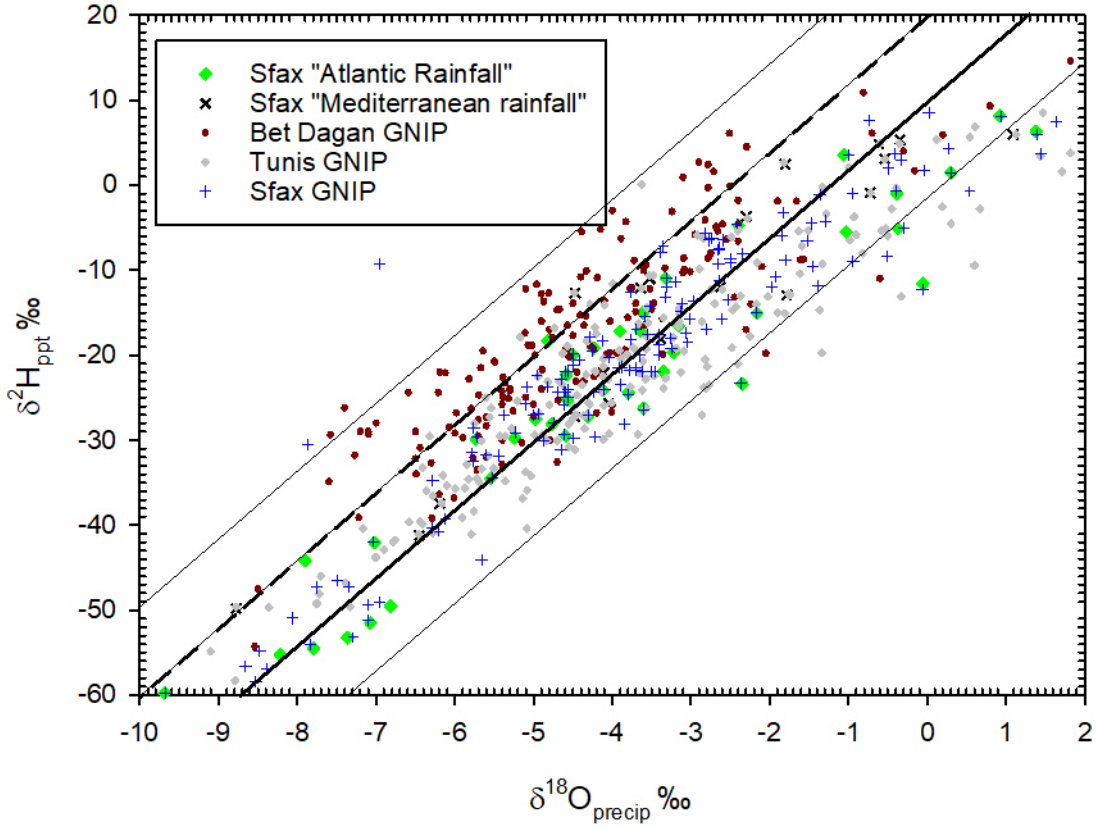

Figure 5b

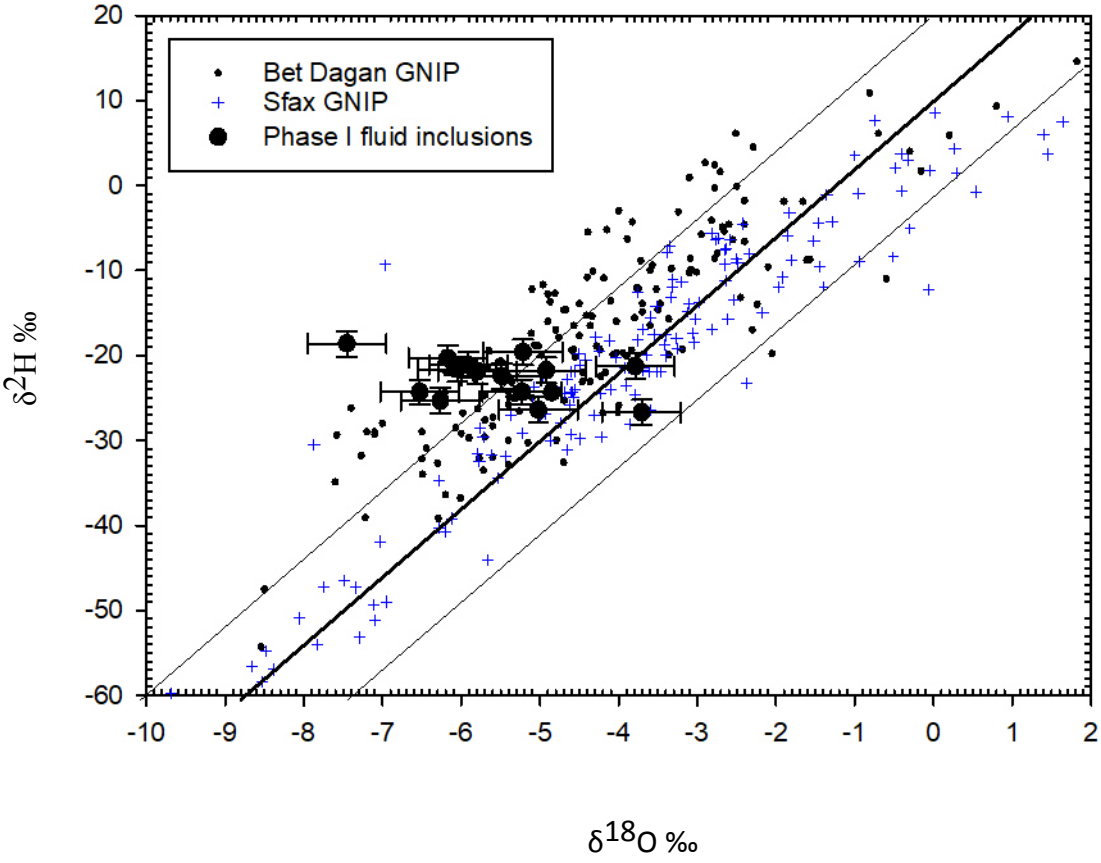

Figure 5c

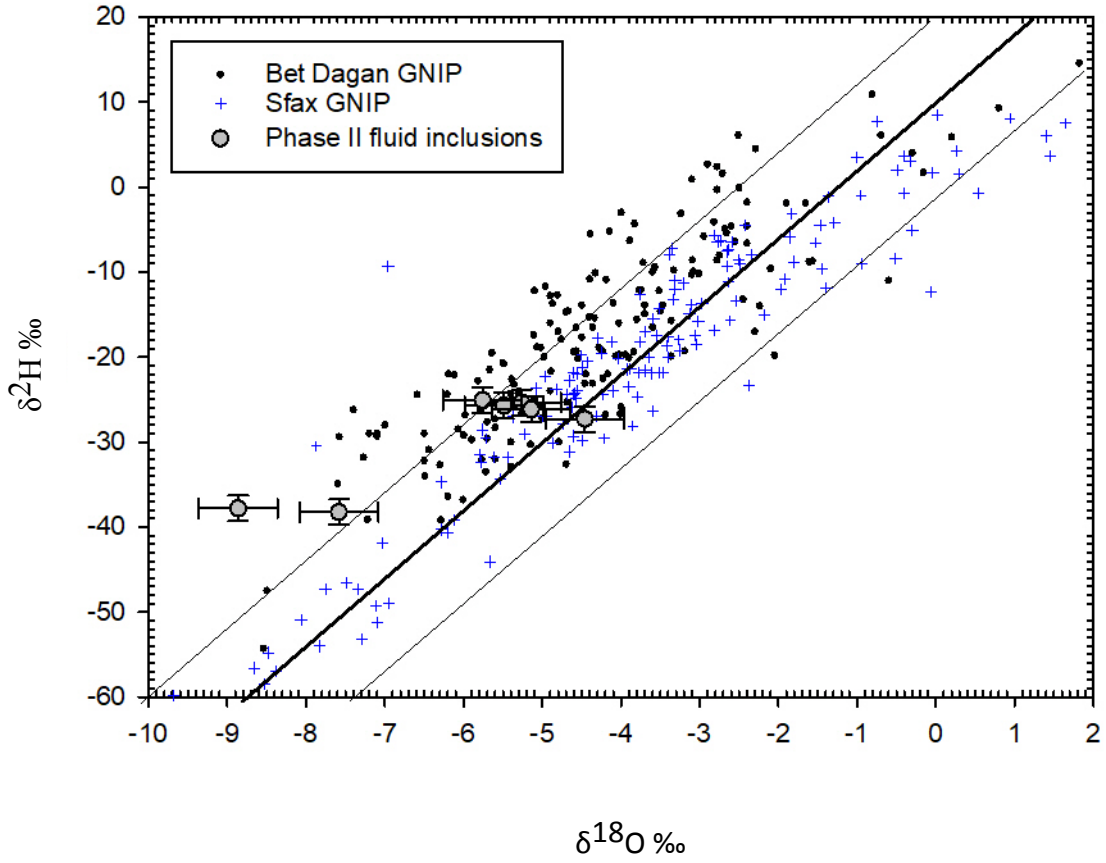

Figure 5d

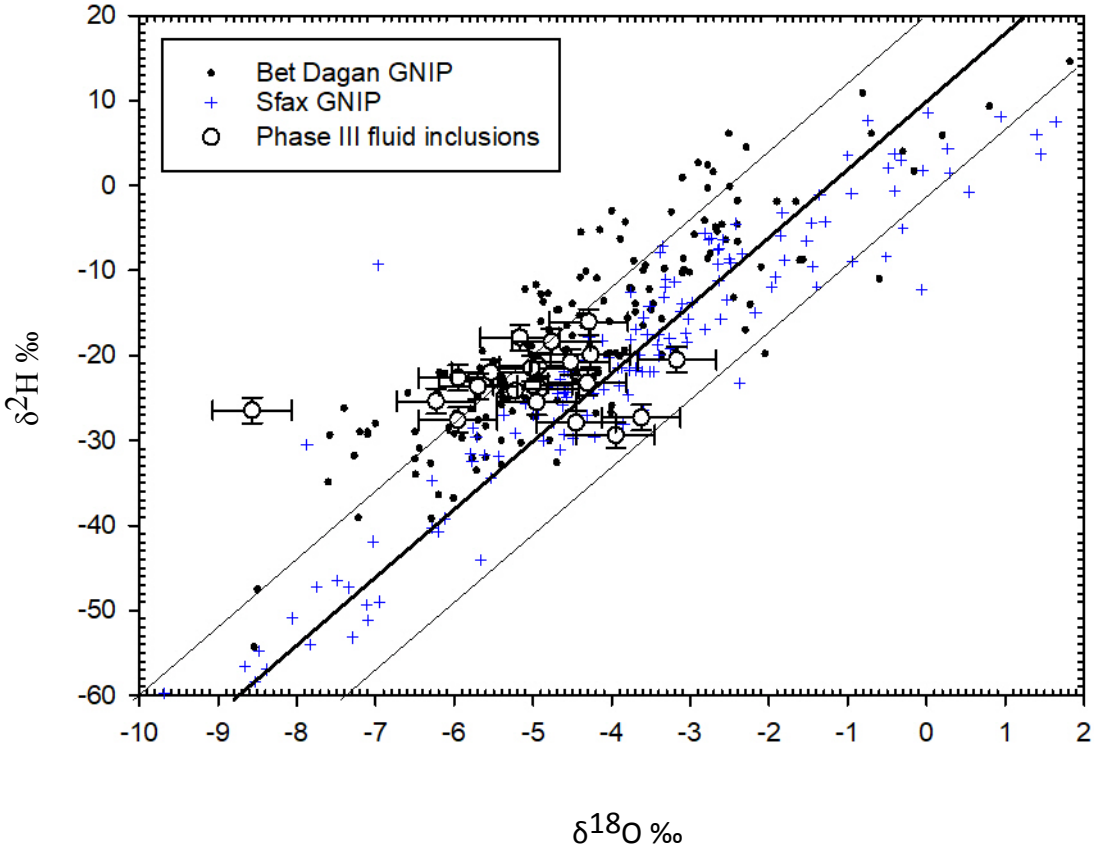

Figure 6

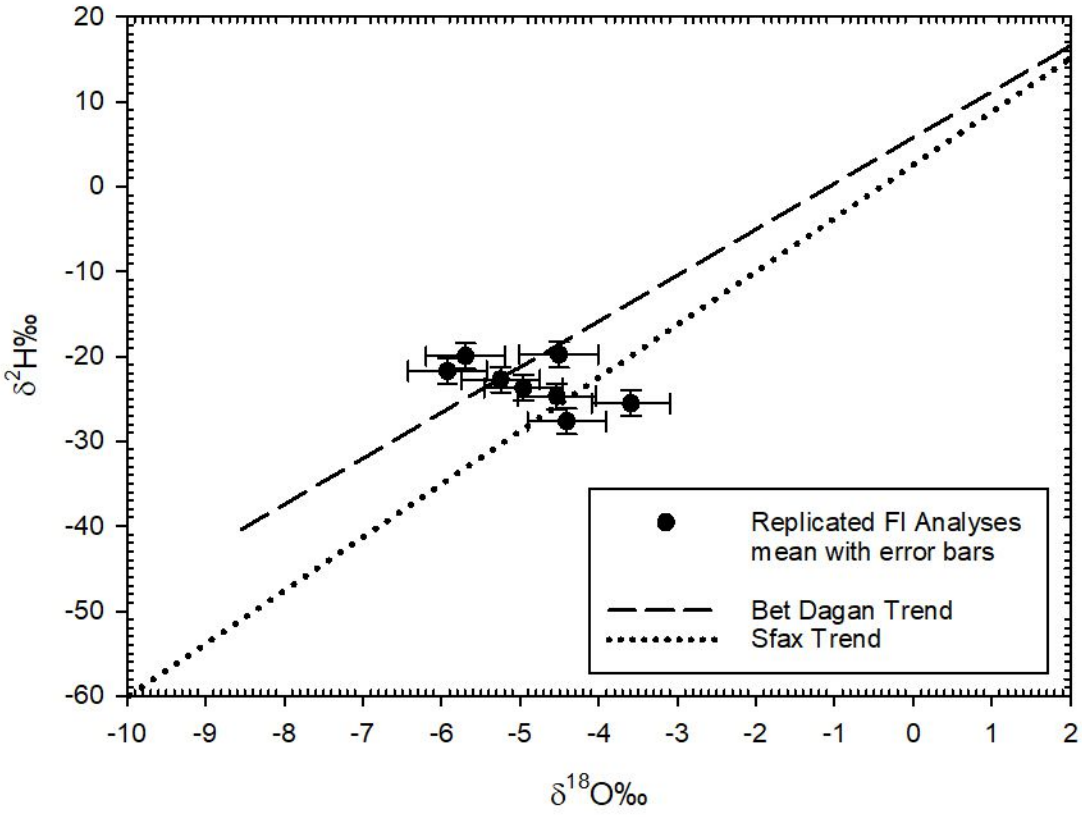
20
10
0
-10
-20
-30
-40
-50
-60
-10
-9
-8
-7
-6
-5
-4
-3
-2
-1
0
1
2
δ2H‰
δ18O‰
Replicated FI Analyses
mean with error bars
Bet Dagan Trend
Sfax Trend

Figure 7

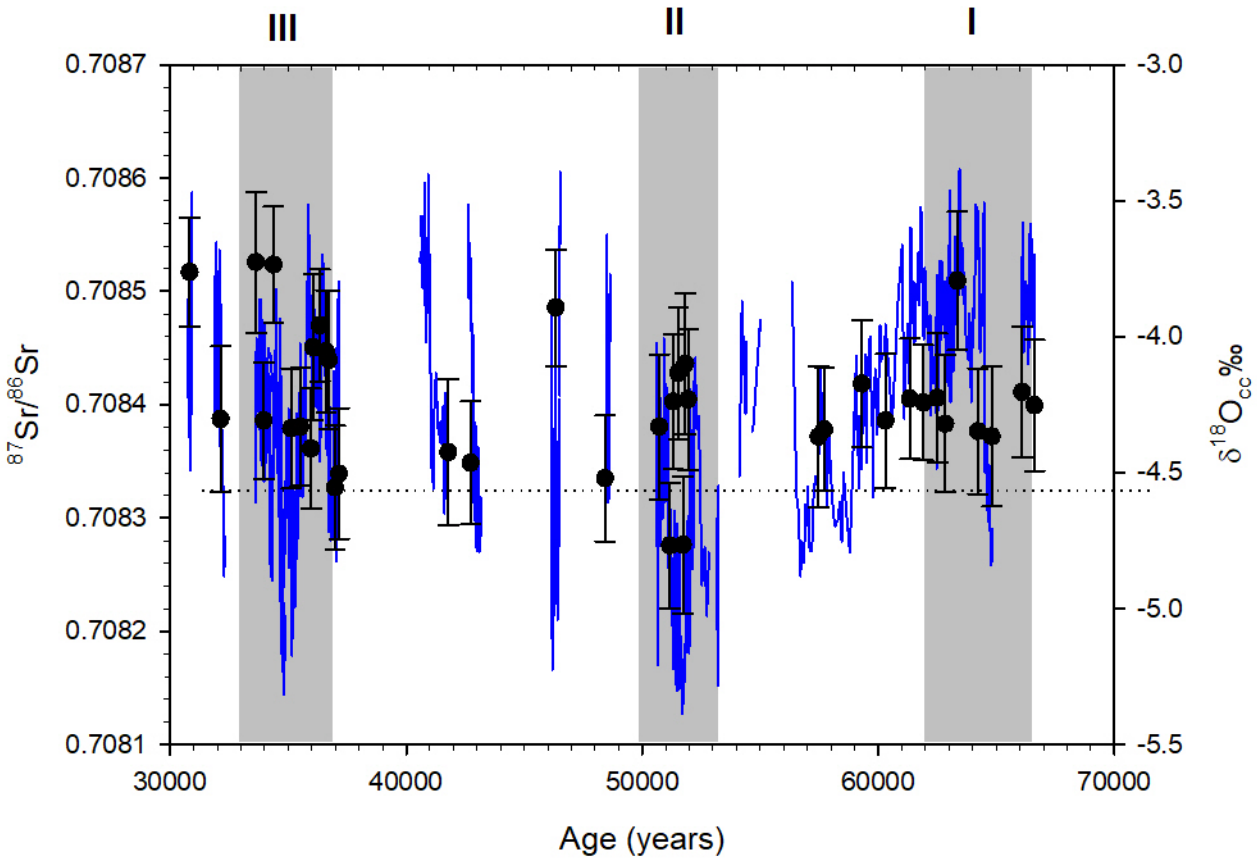
III
II
I
0.7087
0.7086
0.7085
0.7084
0.7083
0.7082
0.7081
$^{87}Sr/^{86}Sr$
-3.0
-3.5
-4.0
-4.5
-5.0
-5.5
$\delta^{18}O_{cc}$‰
30000
40000
50000
60000
70000
Age (years)

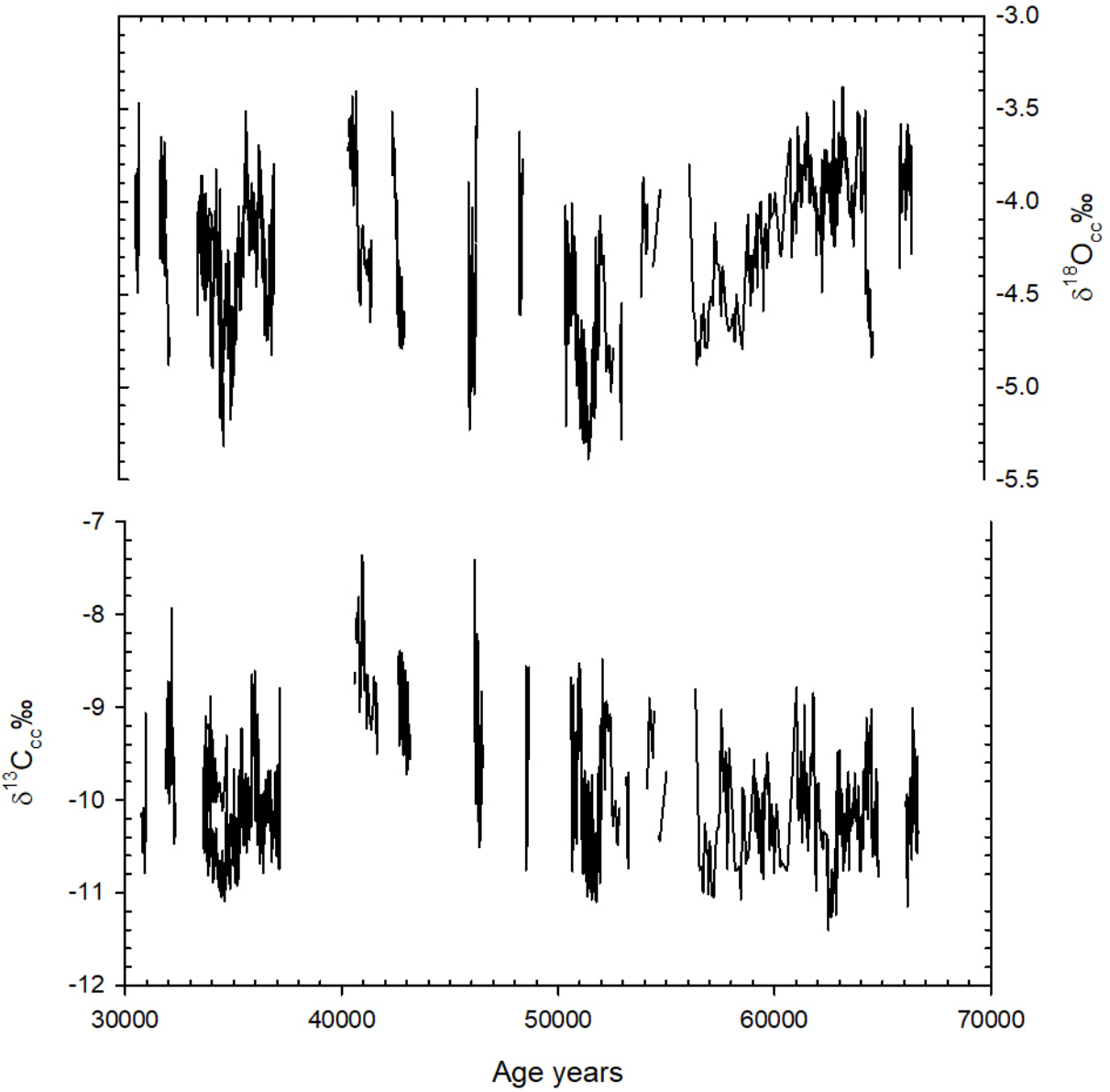
-3.0
-3.5
-4.0
-4.5
-5.0
-5.5
δ18Occ‰
-7
-8
-9
-10
-11
-12
δ13Ccc ‰
30000
40000
50000
60000
70000
Age years

Figure 9

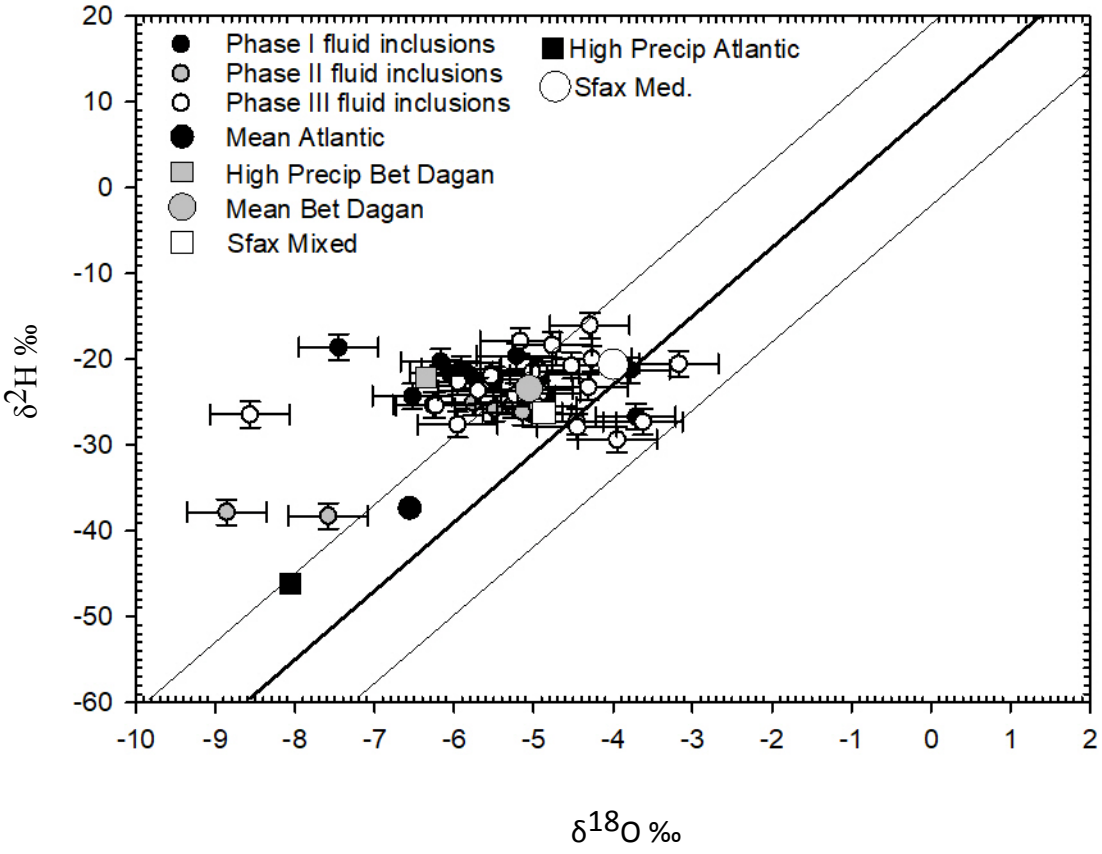
Phase I fluid inclusions
Phase II fluid inclusions
Phase III fluid inclusions
Mean Atlantic
High Precip Bet Dagan
Mean Bet Dagan
Sfax Mixed
High Precip Atlantic
Sfax Med.
δ2H ‰
δ18O ‰
20
10
0
-10
-20
-30
-40
-50
-60
-10
-9
-8
-7
-6
-5
-4
-3
-2
-1
0
1
2

Figure 10

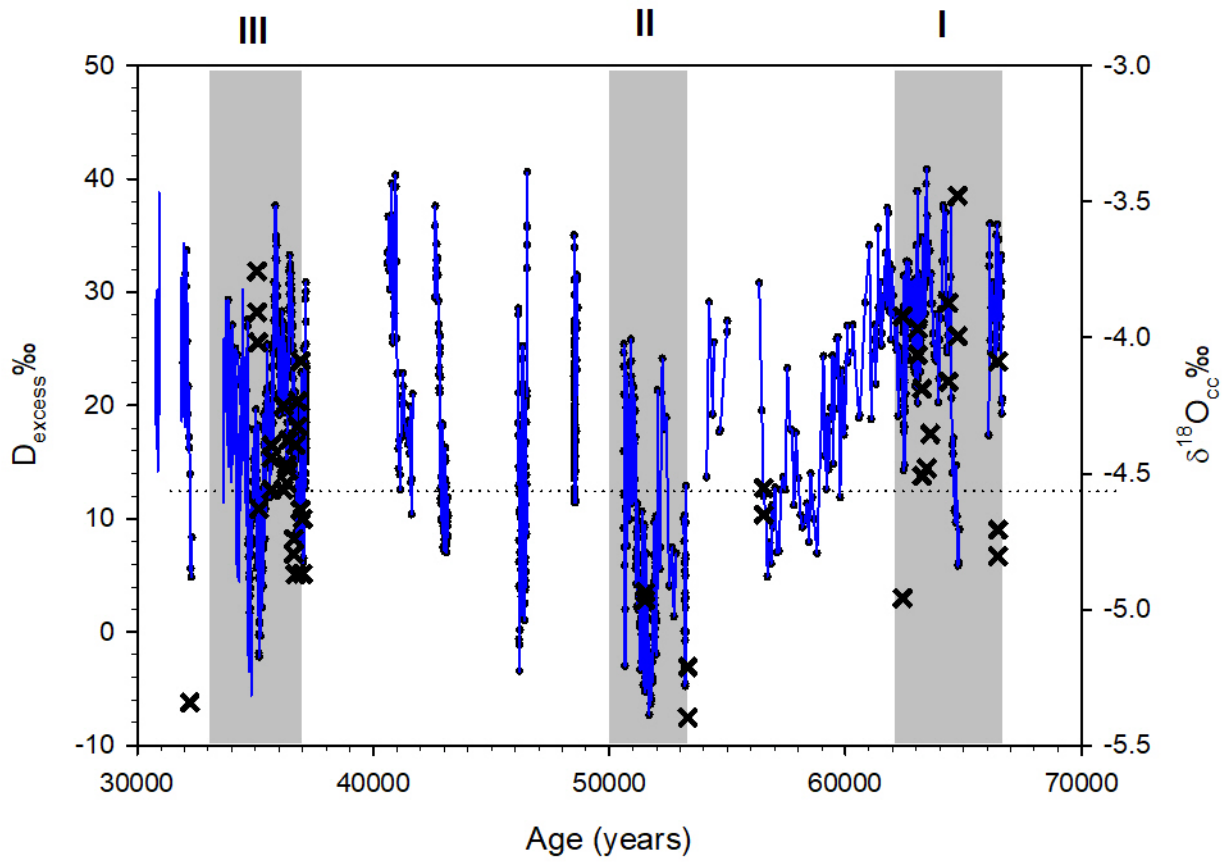
III
II
I
50
40
30
20
10
0
-10
-3.0
-3.5
-4.0
-4.5
-5.0
-5.5
30000
40000
50000
60000
70000
Age (years)
D_{excess} ‰
$\delta^{18}O_{cc}$ ‰